

# Optimization and Design Space Exploration of a Supersonic Business Jet Planform

Josiah T. VanderMey<sup>1</sup> and Hassan J. Bukhari<sup>2</sup>  
*Massachusetts Institute of Technology, Cambridge, MA, 02139*

**A low fidelity, response surface model is used to optimize the wing and tail geometry of a supersonic jet with regard to its profit potential in the business jet market. The model is used to rapidly assess the design space and give preliminary indication as to the performance of such aircraft. Sequential quadratic programming and simulated annealing are considered as optimization techniques. Recommendations for future study are provided.**

## Nomenclature

RSE	= response surface equation
SA	= simulated annealing
SQP	= sequential quadratic programming
SSBJ	= supersonic business jet
$J$	= objective function
$x$	= response surface input variable
$\beta$	= response surface coefficient
$\lambda$	= objective weight factor

## I. Introduction

Starting with the introduction of the Aérospatiale-BAC Concorde in the late 1960's, the vision for a viable supersonic transport aircraft has remained largely unrealized. While a supersonic transport aircraft would provide a significant reduction in travel time, the materials and technologies required to allow for these speed increases incur significant cost penalties over conventional, subsonic jets.<sup>1</sup>

Although the average traveler may be unwilling to pay the increased ticket prices associated with supersonic aircraft, the fast paced lifestyles and deep pockets of business executives allow them to justify more expensive flights. This potential for a sustainable market has directed the focus on supersonic aircraft design to the business jet sector. In addition to its prospective feasibility, the business jet market provides further stability under variable economic conditions as well as extended applications to military, MEDEVAC, and airfreight.<sup>2</sup>

The challenges to designing a profitable SSBJ come with the need to meet strict performance and operating requirements while maintaining sufficiently low acquisition and operating costs. Increased environmental awareness has led to a premium being placed on low emissions and noise pollution. The creation of sonic booms in supersonic flight and the high fuel burn of supersonic engines make these requirements particularly challenging for the SSBJ. Additional performance requirements also constrain SSBJ designs. According to Chudoba et al., a feasible SSBJ should achieve a range of at least 4500 nautical miles with a cruise speed between Mach 1.4 and Mach 1.8.<sup>1</sup> Furthermore, the SSBJ needs to comply with existing regulations and be capable of operating out of a wide range of commercial airports.

This paper describes a preliminary optimization of a SSBJ wing and tail planform geometry with respect to the potential profitability of the vehicle as a supplement to the subsonic business jet market. The optimization is based a low fidelity response surface and performance constraints are used to limit the feasible design space. Although, an optimal design is presented, the limitations of the model and lack of data on the relative importance of the different measures of merit preclude a detailed design from being recommended. Instead, this paper focuses on the techniques used in the optimization. Recommendations are provided for future work.

---

<sup>1</sup> Graduate Research Assistant, Engineering Systems Division

<sup>2</sup> Graduate Research Assistant, Department of Aeronautics and Astronautics

## II. System Model

### A. Model Overview

The system model used in this study takes the wing and tail geometries and engine parameters shown in Table 1 and outputs the performance metrics shown in Table 3 and Table 4. With the exception of the area variables, the planform geometry variables have all been normalized with respect to the wing semi-span.

The model was provided as a “black box” simulation for a supersonic aircraft design. As a result, the assumptions and additional parameters in the model are unknown. Each of the model outputs are defined, as in Eq. (1), by a response surface composed of linear and interaction terms only.

$$RSE = \beta_0 + \sum_{i=1}^n \beta_i x_i + \sum_{i=1}^{n-1} \sum_{j=i+1}^n \beta_{ij} x_i x_j \quad (1)$$

While the RSEs provide very fast function evaluations (on the order of 1e-5 seconds to compute all outputs of a given configuration in MATLAB), they also impose several limitations on the model performance.<sup>3</sup> The first of these limitations is that the accuracy is only guaranteed in a small region around the sampled points. This limitation confines the design space that the model can operate in. The upper and lower bounds shown in Table 1 are used to normalize each of the variables from -1 to +1 in the RSEs. As a result, this model cannot be expected to be a good predictor outside of those bounds.

Since the model RSEs only include first order and interaction terms, the model is also unable to predict local extrema. As a result, we expect any optimal design to have active constraints.

Finally, it is likely that the higher fidelity model behind the RSEs is a computer simulation. Since error is typically not randomly distributed in computer simulations, the RSEs may include some bias.

### B. Model Benchmarking and Validation

Due to the very limited constraints of the RSEs, no existing aircraft designs could be found for comparison that satisfied all of the wing and tail geometry constraints. Nevertheless, two supersonic aircraft with similar mission profiles, the Sukhoi-Gulfstream S-21 and the Aérospatiale-BAC Concorde, were modeled (see Figure 1) and the outputs compared to the actual values in Table 2. The model over predicts the S-21 weight by a factor of about five and gives nonsense values for the Concorde weights and runway distances. These errors are likely due largely to the model extrapolation. The S-21 model violates 9 of the 22 input constraints while the Concorde model violates 12. However, the model may also fail to take into account other aspects of these designs such as canards and delta wing

**Table 1. Model inputs**

Type	Variable	Name	Min	Max
Translation Variables	Wing Apex (ft)	XWING	25	28
	Horizontal Tail Apex (ft)	XHT	82	87.4
	Vertical Tail Apex (ft)	XVT	82	86.4
Planform Geometry Variables	Leading Edge Kink X-Location	X1LEK	1.54	1.69
	Leading Edge Tip X-Location	X2LET	2.1	2.36
	Trailing Edge Tip X-Location	X3TET	2.4	2.58
	Trailing Edge Kink X-Location	X4TEK	2.19	2.36
	Trailing Edge X-Location	X5TER	2.19	2.5
	Kink Y-Location	Y1KIN	0.44	0.58
	Wing Area (ft <sup>2</sup> )	WGARE	8500	9500
	Horizontal Tail Area (ft <sup>2</sup> )	HTARE	400	700
	Vertical Tail Area (ft <sup>2</sup> )	VTARE	350	550
Engine Variables	Nozzle Thrust Coefficient	CFG	0.97	0.99
	Turbine Inlet Temperature (°R)	TIT	3050	3140
	Bypass Ratio	BPR	0.36	0.55
	Overall Pressure Ratio	OPR	18	22
	Fan Inlet Mach Number	FANMN	0.5	0.7
	Fan Pressure Ratio	FPR	3.2	4.2
	Engine Throttle Ratio	ETR	1.05	1.15
	Suppressor Area Ratio	SAR	1.9	4.7
Take-off Thrust Multiplier	TOTM	0.85	1.0	
Thrust-to-Weight Ratio	FNWTR	0.28	0.32	

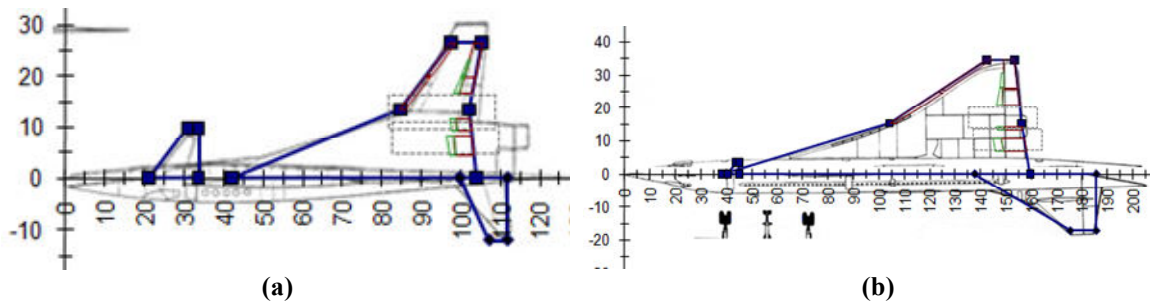


**Figure 1. Model geometries for the (a) Concorde and (b) S-21 overlaid on drawings of their actual planforms**

vortex lift generation. Similarly, the general technology level (materials, construction techniques, etc.) at the time of these designs may have been different than when this model was developed. Consequently, these results are not appropriate for comparison and do not invalidate the model.

Since the model constraints prohibit direct comparison with other aircraft, a baseline configuration at the center of the RSEs was chosen and compared to maximum take-off weight and wing loading trends for supersonic transport aircraft. Figure 3 shows that the maximum take-off weight for the baseline design is on par with other designs. However, from Figure 2 it can be seen that the wing loading of the baseline model configuration is significantly higher. These results do not definitively imply that the model is flawed, however, they are cause for concern and the authors advise that the model formulation and assumptions be more thoroughly validated.

**Table 2. Validation output comparisons**

Type	Output	S21 Model	S21 Act.	Concorde Model	Concorde Actual
Cost	Average Yield per Revenue Passenger Mile (\$/mi)	0.1314		0.105	
	Acquisition Cost (Million \$)	260.28		303.86	350
	Take-off Gross Weight (lbs)	512,090	106,924	807,610	412,000
Performance	Fuel Weight (lbs)	289,560	67,409	2,502,000	210,940
	Take-off Field Length (ft)	19,358	6,495	103,360	11,778
	Landing Field Length (ft)	12,508	6,495	14,024	
	Approach Speed (kts)	185	146	242	
	Approach Angle of Attack (deg)	11.19		12.1	
Feasibility	Fuel Volume Ratio (available/required)	0.58		0.01	
	Delta Sideline Noise	-2.6		24	
Environmental	Delta Flyover Noise	34.9		-207	
	Delta Approach Noise	22.1		-195	

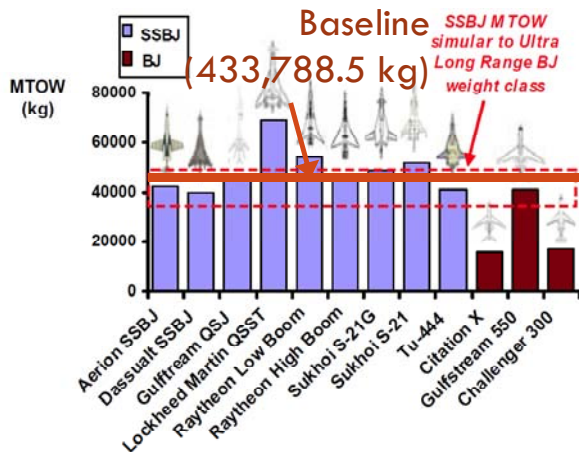


**Figure 3. Maximum take-off weights of several supersonic aircraft.**

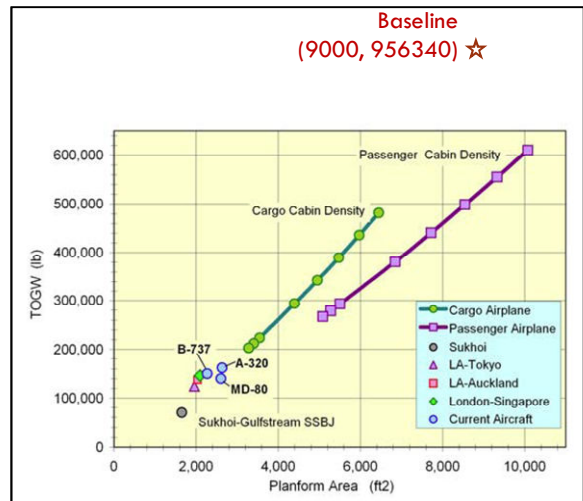


**Figure 2. Wing loading trends for supersonic aircraft.**

### III. Problem Formulation

In accordance with the objective to design a highly profitable SSBJ that complies with noise and performance regulations required to operate out of commercial airports, the optimization approach considered four different objectives that directly contribute to the profitability of a transport aircraft. Table 3 presents these four objectives and their individual optimization goals. Based on these objectives, the market feasibility of the aircraft can be largely determined.

**Table 3. Optimization objectives**

Objective	Name	Direction
Take-off Gross Weight (lbs)	TOGW	Minimize
Fuel Weight (lbs)	FUELWT	Minimize
Average Yield per Revenue Passenger Mile (\$/mi)	DPRPM	Maximize
Acquisition Cost (Million \$)	ACQCST	Minimize

Take-off gross weight is often correlated to aircraft cost as well as size. While cost is already taken into account by a separate objective, minimizing take-off gross weight as an individual objective should result in smaller aircraft that are easier and cheaper to store and maintain.

Fuel weight is important for profitable aircraft because fuel cost is a large component of the aircraft operating cost.

Minimizing fuel weight also helps to mitigate cost risk due to variability in fuel prices.

The average yield per revenue passenger mile is an indicator of the potential profit generation of the aircraft. This number, combined with the expected lifetime and passenger capacity of the aircraft, can be used to determine the expected profit generated by the aircraft.

Finally, acquisition cost reflects the purchase cost of the aircraft. This figure is important not only because it gives the upfront cost of the aircraft, but also because it represents a discrete step size that affects the purchasing schedule of airlines or charter companies who wish to include the aircraft in their inventories.

The output constraints placed on the optimization are shown in Table 4. These constraints are divided into three categories based on whether they are constraints on the performance, constraints on the design feasibility, or environmental noise constraints.

The performance constraints include maximum runway length constraints and a constraint on the maximum approach speed. The runway length constraints are meant to guarantee that the aircraft will be able to operate out of a sufficient number of paved airfields around the world. From Figure 4 it can be seen that the global number of paved runways decreases quite rapidly for lengths exceeding 2,437 m (approximately 8,000 ft)<sup>4</sup>. It would be nice for the aircraft to be able to utilize the maximum number of runways, however, at a minimum the aircraft needs to be able to operate out of the large, major airports. Thus, the upper bound on runway length was set to 11,000 ft.

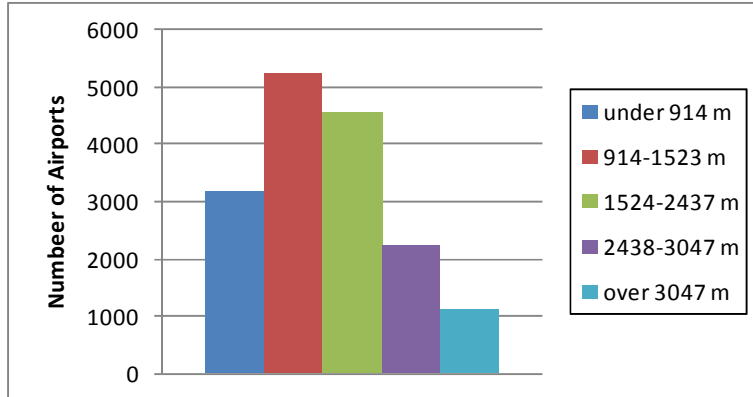


Figure 4. Number of worldwide paved airports by length<sup>4</sup>

Although, as shown in Figure 6, some of the engine parameters can have a significant effect on the aircraft performance, in order to simplify the problem only the 12 geometry and translation variables were included in the design vector. Additionally, some of the engine parameters, such as nozzle thrust coefficient, cannot be explicitly chosen by the designer. Accordingly, the engine variables were fixed as parameters at the center of the RSEs.

#### IV. Optimization

The weighted sum approach shown in Eq. (2) was used to generate the objective function for optimization. Due to its direct impact on profitability, average yield per revenue passenger mile was weighted most heavily. Fuel weight and acquisition cost were weighted next heavily based on their effects on operating costs and acquisition. Finally, take-off gross weight was weighted the least because of its indirect effect on cost and profits. Each objective was also scaled based on the baseline configuration to be  $O(1)$ .

Table 4. Optimization output constraints

Type	Variable	Name	Min	Max
Performance Constraints	Take-off Field Length (ft)	TOFL		11,000
	Landing Field Length (ft)	LANDFL		11,000
	Approach Speed (kts)	APPSPD		155
Feasibility Constraints	Approach Angle of Attack (deg)	AANGLA		12
	Fuel Volume Ratio (available/required)	FRATIO	1.0	
Environmental Constraints	Delta Sideline Noise	SNOISE		10
	Delta Flyover Noise	FNOISE		10
	Delta Approach Noise	ANOISE		10

The approach speed of the aircraft was selected as a constraint because it determines the approach category. Constraining the approach speed to 155 knots ensures that the aircraft will be Category D or lower which sets an upper bound on the landing distance and circling radius.<sup>5</sup>

Approach angle of attack and fuel volume ratio are simply feasibility constraints that ensure that the aircraft has sufficient internal volume and does not stall on takeoff or landing. While the performance constraints are somewhat subjective, violating either of these constraints would result in an inoperable aircraft.

$$J = 0.20 \frac{TOGW}{750000} + 0.25 \frac{FUELWT}{400000} - 0.30 \frac{DPRPM}{0.12} + 0.25 \frac{ACQCST}{230} \quad (2)$$

### A. Design Space Exploration

Because of the relatively large size of the design vector, a Latin Hypercubes experiment was conducted on the 12 design variables as an initial exploration of the design space. 10,000 levels were used in the experiment; however, only three of the evaluations yielded configurations that satisfied all of the output constraints. In particular, each invalid design violated the take-off length and/or the approach noise constraints. The three feasible configurations from the experiment as well as the best designs for each of the individual objectives (including infeasible designs) are presented in Figure 5.

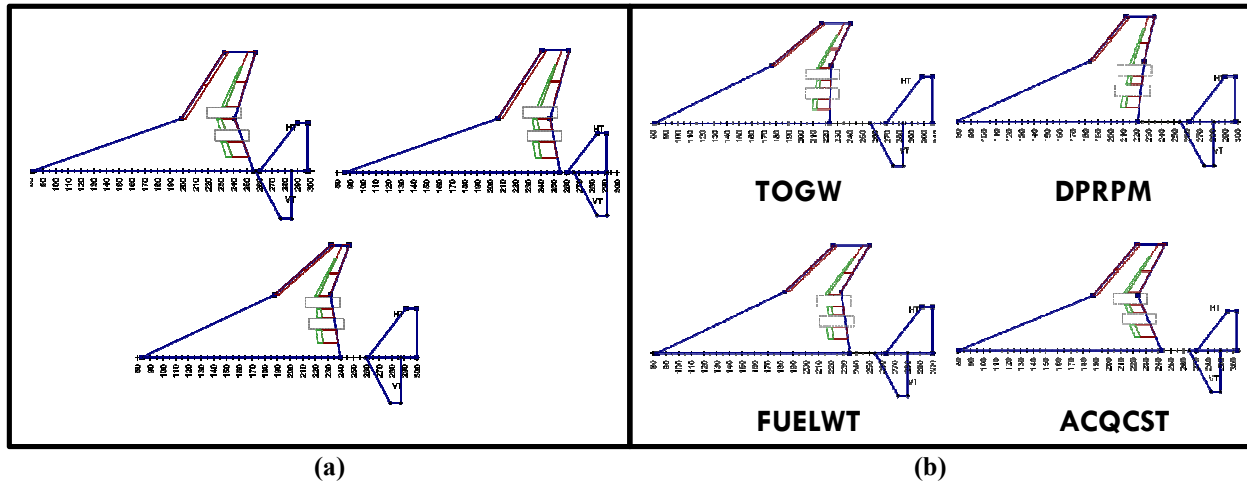


Figure 5. (a) Feasible configurations and (b) best configurations for each objective

The lack of feasible designs implies a highly constrained design space. Such design spaces are often difficult to optimize as gradient methods can become stuck in local minima or islands of feasibility and heuristic methods must be able to deal with frequent constraint violation.

As an additional means of understanding the design space, the main effects of each variable and parameter were computed from the first order coefficients in the RSE's Figure 6 shows a normalized plot of these effects. Based on this information, it appears that the leading edge kink location and the leading edge tip location have the greatest influence on the objective outputs.

### B. Gradient Based Optimization

Since the objective function is modeled by a response surface, gradient methods should be very efficient and converge quickly to the optimal design. Due to its ability to handle nonlinearities, its potential for fast convergence, its suitability for long running simulations, and its widespread acceptance and use in engineering problems, Sequential Quadratic Programming (SQP) was selected as the initial gradient optimizer. The optimization was implemented by means of MATLAB's `fmincon` function.

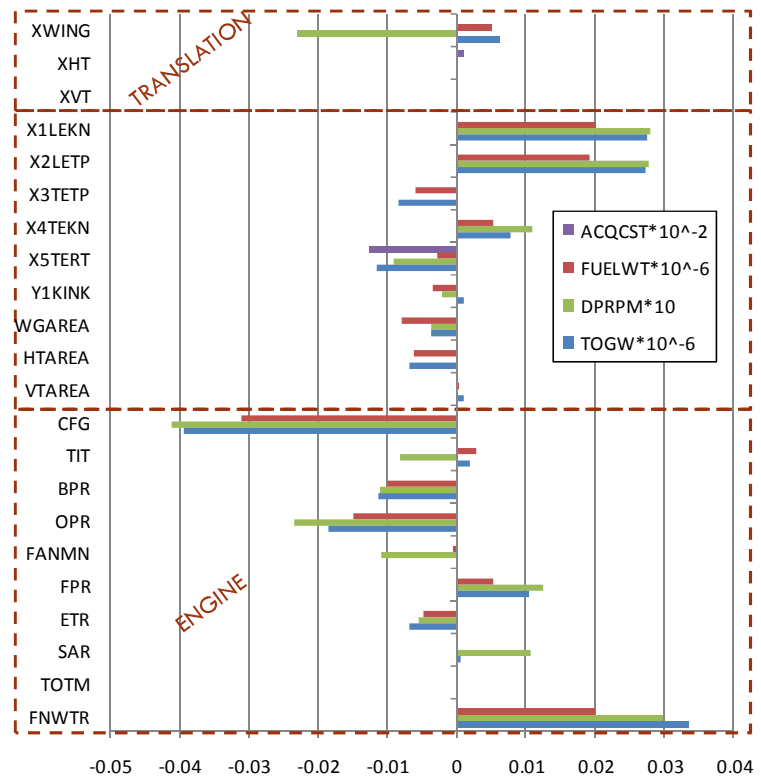


Figure 6. Normalized main effects.

The initial convergence tolerance was set to 1e-6 on both the constraints and the objective function. The seven designs shown in Figure 5 from the Latin Hypercubes experiment were used as starting points for the optimization. Although each optimization converged very quickly, the optimized designs did not show significant improvement over their respective starting points. Similarly, each starting point resulted in a different optimal design.

Constraint tolerances were increased to 1e-12 and the maximum step size was decreased in an attempt to mitigate the potential effects ill conditioned constraints. However, the results did not show significant improvement. These features confirm the results of the Latin Hypercubes experiment in that the design space is highly constrained with islands of feasibility and numerous local optima on the constraint boundaries. Such problems are often better suited to heuristic optimization techniques.

### C. Heuristic Optimization

A simulated annealing method was implemented in MATLAB as a second optimization technique. Simulated annealing allows the optimization to escape local minimums while the temperature is high, but then capitalizes on the low curvature and smoothness of the RSEs by performing similar to a gradient method as the temperature cools. The initial temperature for the optimization was set to 150 and an exponential cooling schedule with a decay rate of

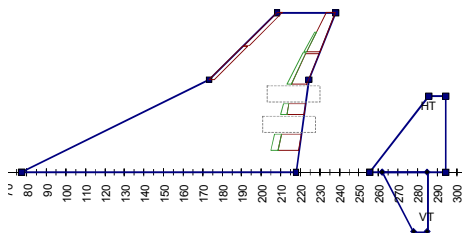


Figure 7. SA optimal design geometry.

0.95 was used. The design perturbation was configured such that four variables were perturbed at each iteration. The perturbation magnitude and direction were selected randomly from a normal distribution with a standard deviation of one third of the allowable range of each variable. Variables that exceeded the input constraints were reset to the boundary. Constraints were handled by a quadratic penalty function where the penalty was set to 1e5.

Although runtimes were significantly longer, the SA optimization yielded much more stable

Table 5. SA optimal design configuration. Active constraints in red.

Type	Variable	Value	Min	Max
Translation Variables	Wing Apex (ft)	25	25	28
	Horizontal Tail Apex (ft)	82.5	82	87.4
	Vertical Tail Apex (ft)	84.5	82	86.4
Platform Geometry Variables	Leading Edge Kink X-Location	1.54	1.54	1.69
	Leading Edge Tip X-Location	2.1	2.1	2.36
	Trailing Edge Tip X-Location	2.58	2.4	2.58
	Trailing Edge Kink X-Location	2.36	2.19	2.36
	Trailing Edge X-Location	2.26	2.19	2.5
	Kink Y-Location	0.58	0.44	0.58
	Wing Area (ft <sup>2</sup> )	9011	8500	9500
	Horizontal Tail Area (ft <sup>2</sup> )	700	400	700
Vertical Tail Area (ft <sup>2</sup> )	350	350	550	

Table 6. SA optimal design outputs. Active constraints in red.

Type	Output	Optimized
Cost	Average Yield per Revenue Passenger Mile (\$/mi)	0.1584
	Acquisition Cost (Million \$)	260.47
	Take-off Gross Weight (lbs)	832,412
Performance	Fuel Weight (lbs)	438,237
	Take-off Field Length (ft)	10,872
	Landing Field Length (ft)	8,485
	Approach Speed (kts)	143.9
Feasibility	Approach Angle of Attack (deg)	10.43
	Fuel Volume Ratio (available/required)	1.35
Environmental	Delta Sideline Noise	9.21
	Delta Flyover Noise	9.92
	Delta Approach Noise	8.54

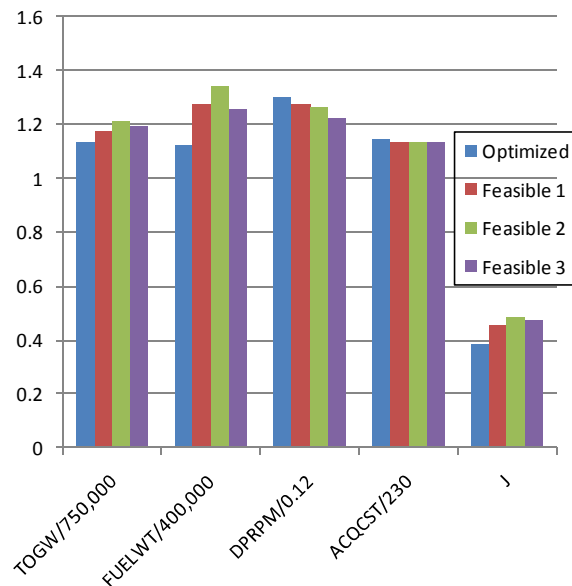


Figure 8. Optimal design improvement.

solutions than the gradient method. Solutions started from multiple locations consistently converged to the design shown in Figure 7 and described by Table 5. Although global optimization is not guaranteed, this consistency over multiple runs with random variable perturbation started from different a different seed point each run gives increased confidence that this is a global optimum. The outputs at the optimized design are presented in Table 6. At the optimized design, the objective function value is 0.3827.

As expected, the solution is highly constrained. 8 of the 12 input constraints are active and 2 of the 9 output constraints are active.

Comparing the optimized design to the three feasible starting points, as in Figure 8, shows a 20% or greater reduction in the objective function value. Furthermore, in addition to improving the overall objective function, the optimized solution improves on all of the individual objectives except for acquisition cost.

#### D. Multiobjective Optimization

Since the weights in the objective function were chosen with limited input from potential buyers or users, it is important to take a step back and look at the optimization from a multiobjective perspective. As a first step in this process, simulated annealing was used to solve for the optimal design using each of the individual objectives as the objective function. Figure 9 shows the optimized geometries. It can be seen that the minimum takeoff gross weight and minimum acquisition cost designs are very similar. This correlation is expected and, to some extent, helps to further validate the model. It is also interesting to note that the optimal design from the previous section resembles the minimum fuel weight design.

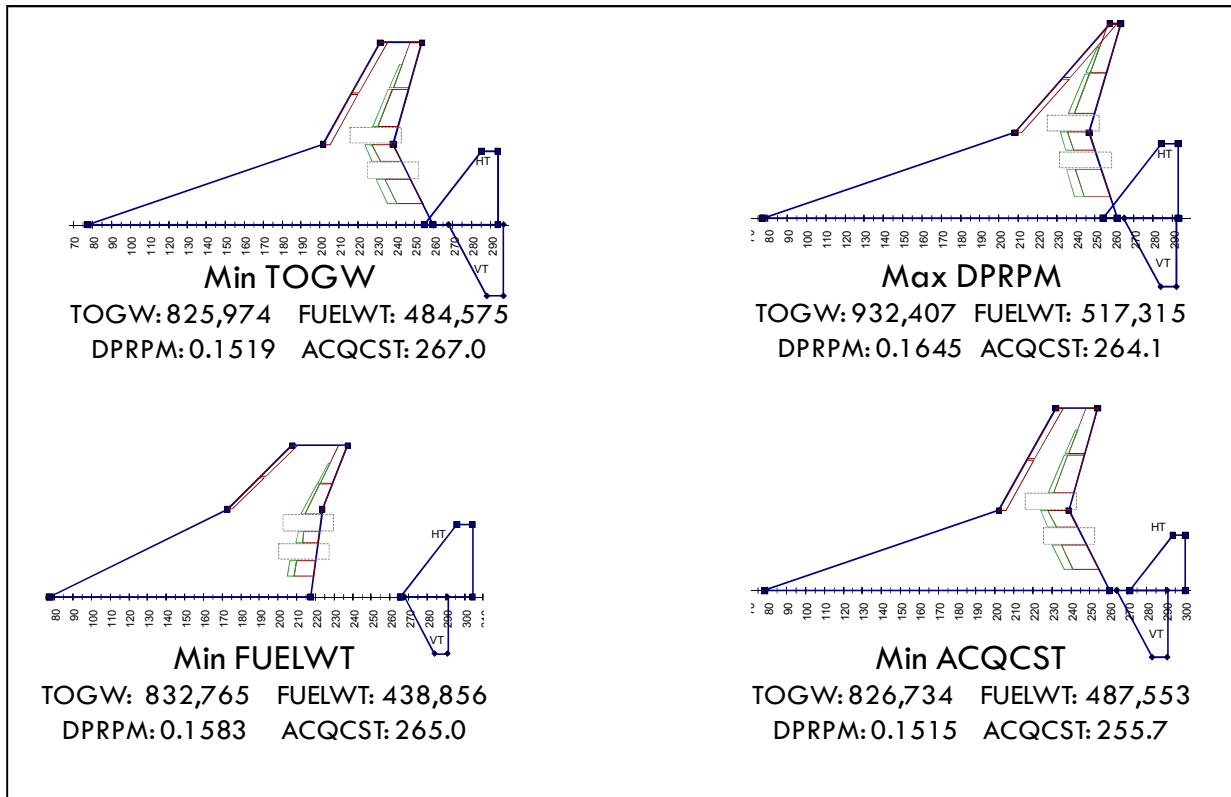


Figure 9. Single objective optimized designs.

Of the individual objectives, minimum take-off gross weight, minimum acquisition cost, and minimum weight are all mutually supporting objectives. The trades occur with these objectives and maximum average yield per revenue passenger mile. In order to understand this trade, a Pareto front estimate shown in Figure 10 was constructed for take-off gross weight and average yield per revenue passenger mile. The Pareto front estimate was constructed using simulated annealing and a weighted sum method, as in Eq. (3), and later improved with an adaptive weighted sum method to fill in some gaps.

$$J = \lambda \frac{TOGW}{750000} - (1 - \lambda) \frac{DPRPM}{0.12} \quad (3)$$

The lack of pronounced convexity in the Pareto front near the middle of the design space means that optimal designs in this region will be highly susceptible to changes in the weighting.

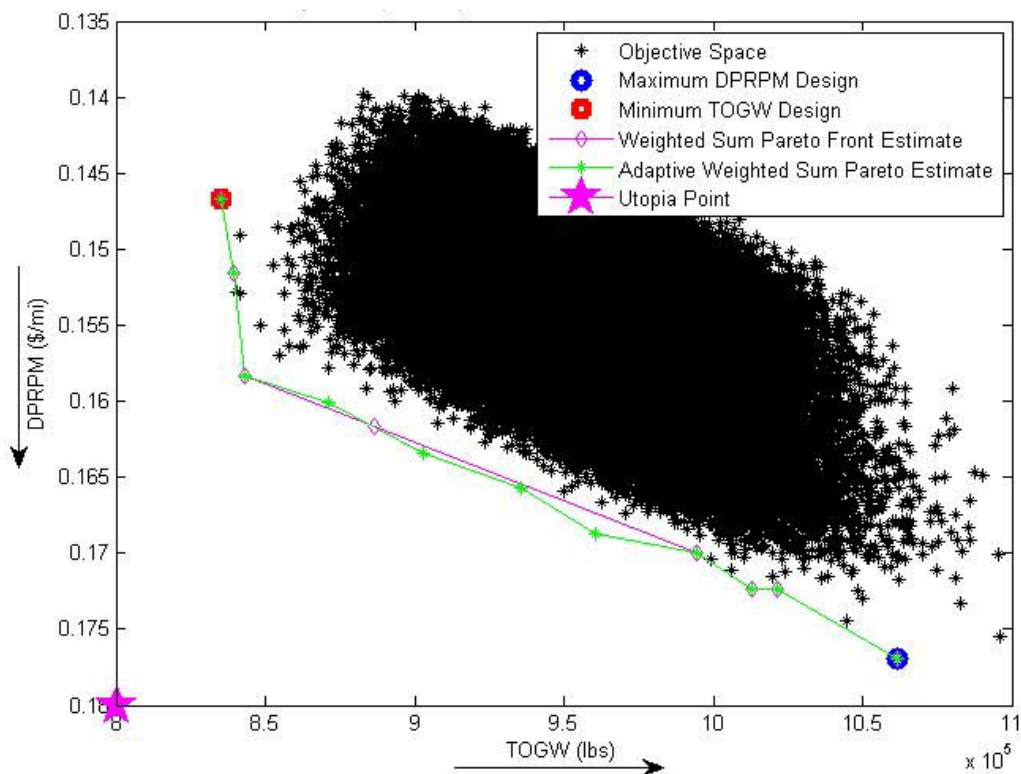


Figure 10. Pareto front estimate for take-off gross weight and average yield per revenue passenger mile.

### E. Post Optimality

Using the RSE's, the sensitivity of the solution to each of the design variables and engine parameters at the optimal design point was computed and graphed in Figure 11. Of the geometry and translation variables, the sensitivity plot shows that the objectives are highly sensitive to the longitudinal leading edge king location, longitudinal trailing edge kink location, and span wise kink location. Accordingly, these are all active input constraints that restrict the design space.

## V. Conclusions and Recommendations

Although an optimal design was selected, the limitations imposed on the optimization make it difficult to recommend this design as the final iteration. More study is needed to refine the design and increase confidence in it.

### A. Model

Due to the lack of insight into the higher fidelity model underlying the response surfaces, additional data is needed to fully validate this model. Because of the unique design space encompassed by the SSBJ, a system level validation may not be possible. However, at the least, each subsystem in the high fidelity model should be validated against know data. Furthermore, the response surface should be evaluated against the high fidelity model at points not included in the regression in order to ensure that the model provides a good fit for the underlying data. It may be helpful to increase the response surfaces to quadratic functions in order to provide more ability to fit the curvature of the high fidelity model.

Because the response surfaces mask the multidisciplinary aspects of the model, it is impossible to determine the assumptions that were made in creating the model. This lack of knowledge significantly restricts the value of the optimization since confidence in optimized designs cannot be evaluated based on their true compliance with

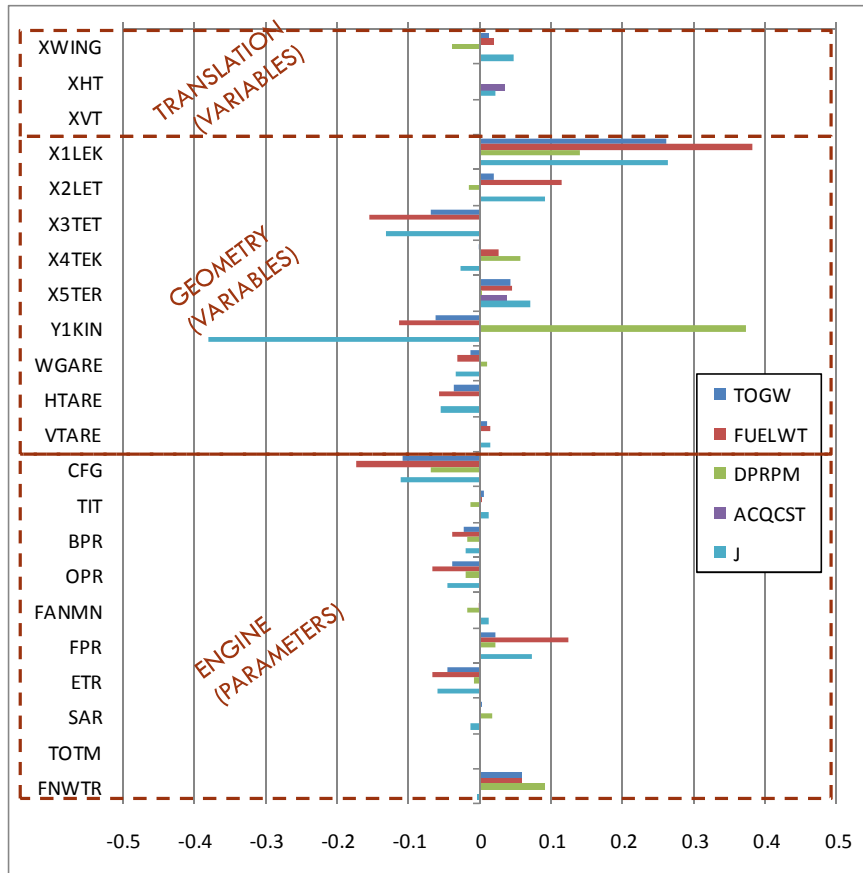


**Figure 11. Normalized sensitivity plot at optimal design point**

results, the optimization is unable to take advantage of the entirety of the available design space. Further refinement of the model at the optimal design point is recommended. Updating the RSE at the optimal design point could allow for the input constraints to be relaxed which, due to the highly constrained nature of the solution, could lead to a substantially better design.

### B. Problem Formulation

Although they were neglected in this study, it is clear that the engine parameters have a significant effect on the aircraft performance. It is recommended that these parameters be included in future studies. In particular, the objectives appear to be most sensitive to bypass ratio, overall pressure ratio, and fan pressure ratio.

It has been shown that the feasible design space is highly restricted by the output constraints. Accordingly, it may also be useful to reconsider the output constraints. In particular, the take-off length and approach noise were the most limiting of the output constraints. While these may be hard constraints, if they could be relaxed it would significantly open up the feasible solution space and allow for better designs. Alternatively, the noise constraints could be converted to objectives depending on exactly how aircraft noise is regulated.

### C. Optimization

Gradient methods, such as SQP, are well suited to RSE's like the system model used here. However, the highly constrained design space prohibits such methods from reaching the global optimum. Since it converges very quickly, the SQP could be started from many locations in the design space in the hopes of obtaining the global minimum in one of the runs. However, as demonstrated by the Latin Hypercubes experiment, even finding a feasible region can be quite difficult. In contrast, simulated annealing is able to move past local minimums to locate the global optimum, but it takes much longer than SQP and becomes very inefficient near the optimal point.

underlying assumptions. Similarly, certain parameter such as speed and altitude that are not known from the RSE models would be useful in the selection of objectives. For example, acquisition cost may be less important for a faster aircraft than it would be for a slower aircraft.

Additionally, the model could be improved to include additional performance metrics and constraints that are not explicitly considered. Stability analysis would provide a good additional constraint. Direct emissions calculations, range, altitude, speed, and drag profiles would also be useful objectives as the aircraft must be able to meet certain performance requirements in order to be feasible in the business jet market.<sup>1</sup>

In its current state, the model is very low fidelity. Additionally, the restricted domain of the RSEs limits the optimization results. Since extrapolation yields poor

These characteristics suggest the use of a hybrid approach in which the SA method is used for several cooling cycles to locate the region of the design space containing the global optimum. Once this region has been located, the SA would pass the optimization to a gradient, SQP solver to quickly converge on the optimized solution

### References

- <sup>1</sup>B. Chudoba & Al., “What Price Supersonic Speed ? – An Applied Market Research Case Study – Part 2”, AIAA paper, AIAA 2007-848, *45th AIAA Aerospace Sciences Meeting and Exhibit, Reno, 2007*.
- <sup>2</sup>Briceño, S.I., Buonanno, M.A., Fernández, I., and Mavris, D.N., “A Parametric Exploration of Supersonic Business Jet Concepts Utilizing Response Surfaces,” AIAA-2002-5828, 2002.
- <sup>3</sup>Chung, H.S., Alonso, J.J., “Comparison of Approximation Models with Merit Functions for Design Optimization,” *AIAA 2000-4754*, 200.
- <sup>4</sup>Field Listing, Airports with Paved Runways," *CIA: The World Factbook, United States of America Central Intelligence Agency*, URL: <https://www.cia.gov/library/publications/the-world-factbook/fields/2030.html> [cited 9 May 2010]
- <sup>5</sup>“Instrument Procedures Handbook,” *Federal Aviation Administration*, Skyhorse Publishing, New York, 2008, Chap. 5.
- <sup>6</sup>C. Trautvetter, “Aerion : A viable Market for SSBJ”, *Aviation International News, Vol. 37, No. 16, 2005*.
- <sup>7</sup>Deremaux, Y., Nicolas, P., Négrier, J., Herbin, E., and Ravachol, M., “Environmental MDO and Uncertainty Hybrid Approach Applied to a Supersonic Business Jet,” AIAA-2008-5832, 2008.
- <sup>8</sup>Federal Aviation Administration (FAA), “Federal Aviation Regulations (FAR)”, FAR91.817
- <sup>9</sup>Cox, S.E., Haftka, R.T., Baker, C.A., Grossman, B.G., Mason, W.H., and Watson, L.T., “A Comparison of Global Optimization Methods for the Design of a High-speed Civil Transport,” *Journal of Global Optimization, Vol. 21, No. 4, Dec. 2001, pp. 415-432*.
- <sup>10</sup>B. Chudoba & Al., “What Price Supersonic Speed ? – A Design Anatomy of Supersonic Transportation– Part 1”, AIAA paper, AIAA 2007-848, *45th AIAA Aerospace Sciences Meeting and Exhibit, Reno, 2007*.

MIT OpenCourseWare  
<http://ocw.mit.edu>

ESD.77 / 16.888 Multidisciplinary System Design Optimization  
Spring 2010

For information about citing these materials or our Terms of Use, visit: <http://ocw.mit.edu/terms>.